HHS Public Access

Author manuscript

Chem Mater. Author manuscript; available in PMC 2021 February 17.

Published in final edited form as:

Chem Mater. 2020 June 23; 32(12): 5208–5216. doi:10.1021/acs.chemmater.0c01307.

Simultaneous Interpenetrating Polymer Network of Collagen and Hyaluronic Acid as an *In Situ*-Forming Corneal Defect Filler

Fang Chen,
Department of Ophthalmology, Stanford University School of Medicine, Stanford, California 94305, United States; VA Palo Alto, Palo Alto, California 94304, United States

Peter Le,
Department of Ophthalmology, Stanford University School of Medicine, Stanford, California 94305, United States; VA Palo Alto, Palo Alto, California 94304, United States

Krystal Lai,
Department of Ophthalmology, Stanford University School of Medicine, Stanford, California 94305, United States

Gabriella M. Fernandes-Cunha,
Department of Ophthalmology, Stanford University School of Medicine, Stanford, California 94305, United States

David Myung
Department of Ophthalmology, Stanford University School of Medicine, Stanford, California 94305, United States; Department of Chemical Engineering, Stanford University, Stanford, California 94305, United States; VA Palo Alto, Palo Alto, California 94304, United States

Abstract

Timely treatment of corneal injuries injury can help to prevent corneal scarring, blindness, and the need for corneal transplantation. This work describes a novel hydrogel that can fill corneal defects and assist in corneal regeneration. This hydrogel is a simultaneous interpenetrating polymer network (IPN) composed of collagen cross-linked *via* strain-promoted azide–alkyne cycloaddition reaction and hyaluronic acid cross-linked *via* thiol–ene Michael click reaction. The formation of the IPN gel was confirmed *via* FTIR spectra, UV–vis spectra, and morphological changes. We compared the gelation time, mechanical properties, transmittance, and refractive index of the IPN gel to the collagen gel, hyaluronic acid gel, and semi-IPN gel. The IPN combined the advantages of collagen and hyaluronic acid gels and supported corneal epithelial cell growth on its surface. When applied to corneal stromal defects *in vivo*, the IPN avoided epithelial hyperplasia, decreased stromal myofibroblast formation, and increased tight junction formation in the regenerated epithelium.

Corresponding Author djmyung@stanford.edu.

Author Contributions

The manuscript was written through contributions of all authors. All authors have given approval to the final version of the manuscript.

The authors declare the following competing financial interest(s): The authors Fang Chen, Gabriella M. Fernandes- Cunha, and David Myung have a patent application pending on the subject of this paper, and David Myung holds on a patent on the smartphone-based ophthalmic camera used in the animal studies.

GRAPHICAL ABSTRACT

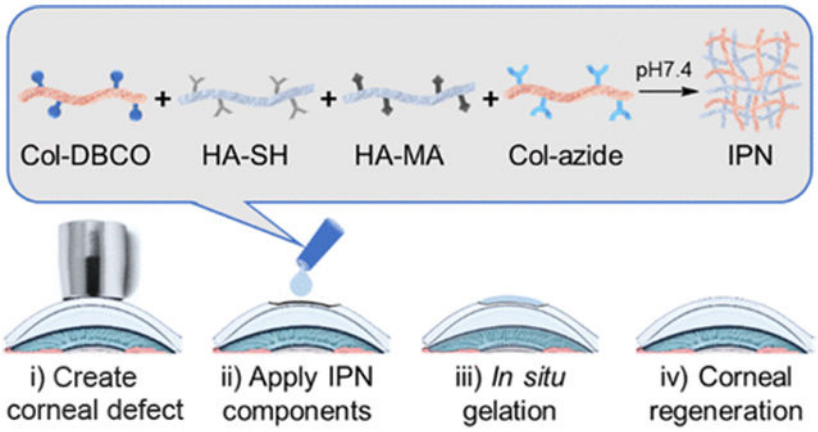

1. INTRODUCTION

In spite of their success in treating corneal blindness, corneal transplants carry inherent risks of graft rejection, infection, and dehiscence with even minor trauma.[1,2] Biomaterials of various kinds have shown promise as corneal substitutes with the potential to address the severe shortage of donor corneas worldwide. Many biomaterials have been investigated for corneal wound healing.[3-7] Preformed hydrogels have been explored extensively over the past two decades but require precise sizing and suturing, among other technical challenges. *In situ*-forming, transparent hydrogels that flow onto and then gel on the cornea hold promise as an alternative to off-label use of opaque cyanoacrylate glue to suturelessly stabilize corneal wounds and have the potential to not only improve vision but also regenerate an overlying epithelium.[3] To this end, bio-orthogonal cross-linking methods such as certain forms of click chemistry are especially promising because they form gels on the cornea without interfering with native biochemical processes and require no external catalyst or energy source such as light or heat.[3] However, there are currently no *in situ*-forming biomaterials available that are specifically approved for the regeneration of wounded corneal tissue. Therefore, efforts are still needed to develop ideal biomaterials for sutureless corneal repair.

In this paper, we report on the development and characterization of a simultaneous (one-pot) interpenetrating polymer network (IPN) hydrogel of hyaluronic acid (HA) and collagen (Col) and evaluate its potential as a corneal defect filler. HA and Col were chosen because they are natural macromolecules and are key components of mammalian connective tissues. HA is a linear polysaccharide that has been widely used in ophthalmic surgery, arthritis treatment, scaffolds for wound healing, dermal filling, and tissue augmentation.[8,9] Its chemical modifications, processing, polymerization, and bioapplications have been intensively investigated.[10] With its robust track record of clinical use, HA is an excellent candidate for implant materials to fill corneal defects by virtue of its versatility, excellent transparency, and biocompatibility. It has been investigated extensively for its capacity to facilitate corneal re-epithelialization, downregulate inflammatory cytokines, and upregulate repair factors.[11,12] We recently reported on the enhancing role that HA can play on corneal

epithelial wound healing in conjunction with secreted growth factors[13] and also developed an *in situ*-forming HA gel cross-linked *via* thiol–ene chemistry.[14]

Collagen has been broadly used in biomedical applications such as bioprosthetic implants, vascular grafts, wound dressings, nerve regeneration, plastic surgery, and drug delivery.[15] Col type I is the primary extracellular matrix component of the corneal stroma. Various forms of Col have been studied extensively as a scaffold material for tissue regeneration. For example, human Col type III-based implants have been reported to improve visual functions of patients with ulcerated or scarred corneas caused by severe infections.[5] A Col derivative, gelatin, has also shown great promise as a structural component of photo-cross-linkable hydrogels, facilitating stromal regeneration and corneal re-epithelialization.[4,6] We previously reported on the development of Col type I hydrogels cross-linked *via* strain-promoted azide–alkyne cycloaddition (SPAAC) reaction and demonstrated their capacity to support multilayered corneal epithelial cell growth.[3]

Here, to combine the advantageous properties of HA and Col in a single *in situ*-forming construct, we have developed an HA–Col hydrogel by creating a simultaneous IPN of independently cross-linked HA and Col without chemical bonding between the two networks.[9] IPNs are able to take on the desirable characteristics of each of their component polymer networks.[16] For example, Naseri *et al.* developed an alginate/gelatin/cellulose-based IPN which showed improved strength comparable to native cartilage for cartilage replacement.[17] Jeon *et al.* improved elasticity and toughness of alginate and gelatin-based hydrogel with an IPN structure for stem cell encapsulation.[18] In this work, we show that the HA–Col IPN hydrogel has certain advantages over HA and Col alone by combining the cell adhesion properties of the Col network while being mechanically strengthened by the presence of the cross-linked HA network.[3,14] The IPN is formed under physiological conditions by mixing thiolated HA (HA-SH), methacrylated HA (HA-MA), azido-modified Col (Col-azide), and DBCO-modified Col (Col-DBCO) at the same time (Scheme 1). Of note, both networks of the IPN are formed simultaneously within the mixture, rather than sequentially as many IPNs reported in the literature are synthesized.[19-21] Moreover, this IPN is formed *in situ* without the need for an external energy source such as light, heat, or a chemical catalyst such as copper or an initiator. We studied the cross-linking, morphology, strength, gelation time, transparency, refractive index, and biocompatibility of the IPN. We also studied the potential of the IPN as an *in situ*-forming corneal stromal defect filler in a rabbit stromal defect model.

2. METHODS

2.1. Materials.

Dibenzocyclooctyne-sulfo-*N*-hydroxysuccinimidyl ester (DBCO-sulfo-NHS), dimethyl sulfoxide (DMSO), sodium hydroxide, agarose, insulin, Triton-X, trypan blue solution, and resazurin based *in vitro* toxicology assay kit were purchased from Sigma-Aldrich (St. Louis, MO, USA). Phosphate-buffered saline (PBS), Col I bovine protein solution (5 mg mL^{-1}), epidermal growth factor (EGF) recombinant human protein, fetal bovine serum (FBS), keratinocyte serum-free media (KSFM), bovine pyruvate extract (BPE), ITS Premix Universal Culture Supplement, trypsin, live/dead viability/cytotoxicity staining kit,

paraformaldehyde (PFA), 5% normal goat serum, Alexa Fluor Phalloidin 488, Alexa Fluor 647-N-hydroxysuccinimidyl ester, Slide-A-Lyzer Dialysis Cassette, and Alexa Fluor 546 secondary antibody were purchased from Thermo Fisher Scientific (Waltham, MA, USA). Azido-poly(ethylene glycol)5-*N*-hydroxysuccinimidyl ester (azido-PEG5-NHS) was purchased from BroadPharm (San Diego, CA, USA). Thiolated hyaluronic acid (HA-SH) and methacrylated hyaluronic acid (HA-MA) were purchased from Blafar Ltd (Dublin, Ireland).

2.2. Hydrogel Synthesis.

Col SPAAC-cross-linked gels (xCol) were synthesized according to our previous publication.[3] First, type I bovine Col was conjugated with either DBCO or azido. Briefly, type-I bovine Col was pH-neutralized using a solution that consists of 1.0 M sodium hydroxide solution, distilled deionized water, and 10× PBS at a 3:57:20 ratio. The neutralization solution was mixed with 5 mg/mL type I bovine Col at a 3:2 ratio to yield 0.3% neutralized Col solution. Then, 8.52 μL of 100 mg/mL DBCO-sulfo-NHS/PBS was added to 1 mL of the neutralized Col solution. The mixture was rotated at 4 °C for 2 h. To make Col-azide, 6.92 μL 100 mg/mL azido-PEG5-NHS in DMSO was quickly mixed with 1 mL of the neutralized Col. The mixture was rotated for 2 h at 4 °C and then dialyzed overnight. For fluorescent Col-azide, the mixture was rotated for another 2 h at 4 °C after adding 8.33 μg of Alexa Fluor 647-*N*-hydroxysuccinimidyl ester before dialysis. To form 0.3% xCol, the as-synthesized Col-DBCO and Col-azide were mixed at 1:1 (v/v) ratio directly at room temperature. To form 0.15% xCol, Col-DBCO and Col-azide were diluted with PBS to 0.15% first. Noteworthy, both Col-DBCO and Col-azide should be made freshly to form xCol.

HA thiol–ene gel (xHA) was made with commercially available HA-SH and HA-MA. Lyophilized HA-SH and HA-MA powders were rehydrated with 7.13× PBS containing 0.0395 M sodium hydroxide to 5%. The rehydrated HA-SH and HA-MA were mixed at 1:1 (v/v) ratio to form 5% xHA. To make 2.5% xHA, the HA-SH and HA-MA were diluted with PBS to 2.5% and then mixed at 1:1 (v/v) ratio.

To make the semi-IPN, we mixed freshly made neutralized Col (0.3%), HA-SH (5%), and HA-MA (5%) solutions at 2:1:1 ratio. The gelling was performed at room temperature without any other catalyst or initiator.

The IPN was made by mixing freshly made Col-azide (0.3%), HA-MA (5%), HA-SH (5%), and Col-DBCO (0.3%) solutions at 1:1:1:1 ratio in order. The mixture was left in an ambient environment to form IPN gel without any other catalysts or initiators.

2.3. Hydrogel Characterization.

The rheological properties of the gels were measured using an ARES-G2 rheometer (TA Instruments, New Castle, DE, USA). *In situ* rheology of the 0.15% xCol, 5% xHA, semi-IPN, and IPN was measured with a 25 mm parallel plate. Time sweeps were measured under 1% strain and 1 Hz oscillatory frequency at 25 °C until the storage modulus plateaued. Frequency sweeps were performed under 1% strain with an oscillatory frequency from 0.1 to

10 Hz at 25 °C. A solvent trap was used during all rheological measurements to prevent samples from dehydrating.

For the Fourier-transform infrared spectra measurement, the samples were each analyzed on a precleaned Diamond ATR crystal using the one-pass ATR attachment and was examined by Fourier transform infrared spectroscopy (Nicolet 6700 spectrometer) in the ATR mode. The spectral resolution is 4 cm^{-1} with a total of 256 scans. For the UV–vis absorbance spectra measurement, the samples were scanned from 270 to 350 nm with a microplate reader (Tecan).

The morphology of the hydrogels was examined with scanning electron microscopy (SEM) (Apreo S LoVac, Thermo Fisher Scientific). The hydrogels were flash-frozen by dipping into a liquid nitrogen tank and then lyophilized immediately. The lyophilized gels were pasted on top of the scanning electron microscope sample holder with silver paste. To increase the conductivity, all samples were sputter-coated with Au/Pd at a 60:40 ratio. The samples were imaged with SEM at 5 kV and 13 pA.

The transmittance of the hydrogels was determined by measuring the absorbance and then calculating with the equation: Transmittance (%) = $1/10^{A} \times 100$, where A represents the measured absorbance. To measure the absorbance, 100 μL of the gels was fabricated in a standard 96-well plate and then scanned with a Tecan microplate reader between the wavelengths of 200–1000 nm. The same volume of double-distilled water was used as a blank. The absorbance was measured on days 0, 1, 3, and 10. The gels were sealed with a parafilm and stored in a cold room to prevent dehydration during this period.

The refractive index of the hydrogels was recorded using a digital refractometer (HI96800, Hanna Instruments). Double-distilled water was used to calibrate the device, and all measurements were normalized to 20 °C. The surface focal power (D_s) of the hydrogels was determined using the equation $D_s = (n - 1)/r$, where n represents the measured refractive index and r represents the radius of curvature. For humans, the radius of curvature is approximately 8 mm.

2.4. Cell Culture and Biocompatibility.

Corneal epithelial cells (ATCC CRL-11135) were used in this study to test the hydrogels' biocompatibility. Cells were cultured in a keratinocyte serum-free medium supplemented with 0.05 mg/mL bovine pituitary extract, 5 ng/mL epidermal growth factor, 500 ng/mL hydrocortisone, and 5 μg/mL insulin. Cells were incubated under the standard conditions and the medium was refreshed every other day. Cells were passaged at 80% confluency with trypsin–EDTA solution.

Biocompatibility of the hydrogels was assessed using both Resazurin assay and calcein AM/ethidium homodimer-I live/dead assay. For the Resazurin-based cytotoxicity assay, 10,000 cells were seeded in 96-well plates and allowed to incubate overnight. The cell media was then replaced with fresh media containing the various hydrogel components. After 4 h of incubation, the cell media were removed and a 1:10 solution of resazurin to cell media was

added to the wells and incubated for another 4 h. The fluorescence was read at 545 nm for the excitation wavelength and 590 nm for the emission wavelength.

For the calcein AM/ethidium homodimer-I live/dead assay, the hydrogels were fabricated on 15 mm diameter glass slides and placed into a 12-well plate. Then, 240,000 cells were seeded on top of the gels. When the cells on the gel were approximately 80% confluent, the cell media were removed and new cell media containing 1:1000 calcein AM and 1:500 ethidium homodimer-I were added. After 45 min of incubation, the cells were imaged using an inverted microscope under the conditions of 37 °C and 5% CO_2. The cell survivability was quantified with ImageJ software.

2.5. *In Vivo* Corneal Defect Model and Treatment.

Adult New Zealand white rabbits were used for *in vivo* studies. Animal experiments were designed to conform with the ARVO statement for the Use of Animals in Ophthalmic and Vision Research and were reviewed and approved by the Stanford University Institutional Animal Care and Use Committee. All anesthesia techniques were performed by the veterinary service center (VSC) at Stanford University. Prior to surgery, one drop of proparacaine hydrochloride ophthalmic solution was added to the experimental eye. A manual lamellar keratectomy was performed on the rabbit corneas using a 3.5 mm customized vacuum trephine to introduce a circular defect, followed by removal of the stromal layer with a blunt spatula. The hydrogel components were mixed in an Eppendorf tube and immediately, 5 μL of the mixture was applied to the defect. The gel was allowed to form on the cornea for around 2 min and then covered with a protective contact lens. Partial tarsorrhaphy was performed to keep the animal from agitating the wound. Ofloxacin ophthalmic solution was applied daily to reduce the risk of infection and to keep the eye moist. Eye examinations were performed on day 4 and day 7. High-resolution photos of the eye were taken with a Paxos smartphone-based ophthalmic camera adapter. Optical coherence tomography (OCT) of the anterior eye segment was carried out with an HRA + OCT Spectralis (Heidelberg Engineering Inc., MA, USA). On day 7, the corneas were collected and fixed in 4% PFA. The fixed cornea tissues were embedded in Tissue-Tek OCT compound and then cryo-sectioned.

2.6. Immunofluorescence.

The fixed samples were washed with PBS thrice and then incubated overnight with primary antibodies alpha smooth muscle actin or zonula occludens-1 in 0.5% triton-x and 5% normal goat serum. The secondary antibody anti-mouse Alexa 546 was added. After washing, the sections were incubated with F-action and DAPI for 50 and 5 min, respectively. The sections were then mounted and imaged with a confocal microscope (Leica TCS SP5).

2.7. Data Analysis.

All data are expressed as the mean ± standard deviation. Each experiment was repeated at least three times unless otherwise indicated. A two-tailed Student's *t*-test was used for significance and p values < 0.05 were considered as significant. Data means, standard deviations, and p values were calculated in Microsoft Excel.

3. RESULTS AND DISCUSSION

3.1. Synthesis.

Four types of hydrogels were synthesized in this study: (1) Col cross-linked *via* SPAAC click reaction (xCol); (2) HA cross-linked *via* thiol–ene click reaction (xHA); (3)a semi-IPN composed of xHA and physically cross-linked Col; and (4) an IPN composed of xHA and xCol. Tissue-extracted Col can form physical cross-links to form gels that are significantly weaker than native tissue Col, which has a well-organized structure.[15] Physically cross-linked Col also exhibits relatively poor transparency, which is undesirable in the substitution of normally crystal-clear corneal stroma. Chemical cross-linking can improve the mechanical and optical properties of tissue-derived Col.[3] Here, we chose to use the SPAAC reaction, which is bio-orthogonal: it does not cross-react with functional groups and biological systems and proceeds under physiological conditions without the need for light, heat, initiator, or a catalyst and produces no side products.[22,23] We modified aliquots of Col with azido and dibenzocyclooctyne (DBCO), which caused the formation of xCol *via* reaction between azido and DBCO groups upon mixing (Scheme 1a). In spite of these cross-links, however, the xCol is still relatively weak because of the lack of fibrillar structure.[15,24]

Native HA also has poor mechanical properties and short residence time because of its fast degradation. An effective way to overcome these limitations is to modify HA and enable cross-linking between HA molecules.[10,25] Herein, we chose thiol–ene click chemistry to cross-link the HA (Scheme 1b) because the thiol–ene click reaction is highly efficient, simple to execute, produces no side products, and proceeds relatively quickly under mild aqueous conditions.[26] The precursors of xHA are thiolated and methacrylated HA, which have shown great potential in corneal wound healing and cell encapsulation. HA-SH has been shown to form films that are reported to promote corneal epithelial wound healing and increase the corneal transparency in a corneal alkali burn rabbit model.[27] HA-MA can cross-link with thiolated heparin *via* visible light-mediated thiol–ene reaction and encapsulate stem cells.[28] Previously, we cross-linked methacrylated and thiolated HA using light-induced thiol–ene click reaction and riboflavin phosphate as the photoinitiator.[14] In this work, to suit the *in situ* application of the final IPN on the cornea and avoid any possible light damage to the eye, we used mildly basic conditions (pH < 8.0) to drive the thiol–ene click reaction without using light or any exogenous chemical catalyst (Scheme 1a).[29]

The formation of the IPN was confirmed by comparing the FTIR spectra and UV–vis absorbance spectra of the IPN to those of xHA, xCol, and the gel components. An S–H signal at 2550 cm^{-1} was only observed from the FTIR spectrum of HA-SH, and a C═C signal at 1620 cm^{-1} was only observed from the FTIR spectrum of HA-MA (Figure 1a).[14] The absence of the S–H and C═C signals in the spectra of the xHA and IPN indicated the cross-linking of thiol and methacrylate groups in these gels. The UV–vis absorbance spectrum of the IPN was also compared to that of xCol and Col-DBCO. DBCO exhibited intense absorbance peaks at approximately 290 and 310 nm,[22] which was also seen in the UV–vis spectra of the Col-DBCO (Figure 1b). The absence of these peaks in the xCol and IPN was due to consumption of the DBCO groups during gel formation as the DBCO reacts with the azide groups.

To ensure a high water content (97.35%) of the IPN and semi-IPN gels for corneal wound healing application, only 2.5% HA and 0.15% Col were used. However, to compare the properties of four gels and study the effect of polymer content on the gel properties, we used different polymer contents as listed in Table 1.

3.2. Rheological Characterizations.

xCol was formed *via* bio-orthogonal SPAAC-based click chemistry reaction as reported previously.[3] To make the azido- and DBCO-conjugated Col, a 2-fold molar excess of azido and DBCO to the amine group of collagen were used, which has been approved to be the most effective condition.[3] To visualize the gel under fluorescence imaging, Col-azide was modified with Alexa Fluor 647 *via* NHS-facilitated amide reaction under physiological conditions. There was 340 nmol Alexa Fluor 647 conjugated onto 1 g of Col-azido as determined by fluorescence quantification. Col-azide (0.3%) and Col-DBCO (0.3%) were mixed at 1:1 (v/v) and started to gel upon mixing, which was indicated by the higher storage modulus than the loss modulus at the first measured time point of the *in situ* rheology measurement (Figure 2a).[23] The storage modulus reached its half maximum within seconds and plateaued in approximately 20 min (Figure 2a).

The xHA was synthesized with HA-SH and HA-MA *via* thiol-Michael-type reaction, which is typically a base-catalyzed thiol–ene click reaction. The thiol-Michael-type reaction is particularly favorable for *in situ* gel application on cornea because of the lack of need for light or photoinitiators because light poses risk for ocular tissue damage and photoinitiators could affect the transmittance of gel.[14] In addition, this reaction produces no byproducts and can be fast with the presence of mildly basic conditions. Although this reaction needs a mildly basic condition, the alkalinity can be very low (pH < 8.0).[30] The degree of substitution of HA-SH and HA-MA was 58% and 43%, respectively. Both HA-SH and HA-MA show a pH of approximately 6.5 after rehydration in PBS. PBS-rehydrated HA-SH (5%) and HA-MA (5%) did not form gels within 24 h upon mixing. Therefore, we studied the base strength and concentration to increase the final pH to approximately 7.1 so that the thiol-Michael reaction could happen to form gels under physiological conditions. This was achieved by rehydrating every milligram of HA-SH and HA-MA with 20 μL 7.13× PBS containing 0.79 μmol sodium hydroxide. The rehydrated HA-SH and HA-MA were mixed at 1:1 (v/v) to form xHA. *In situ* rheology studies showed that the HA-SH and HA-MA started to gel upon mixing and the storage modulus reached half maximum after 22 min and plateaued after 50 min (Figure 2b).

Figure 2c shows the *in situ* rheology of the IPN, which can be considered as half 0.3% xCol and half 5% xHA interpenetrating with each other. The gel started to gel upon mixing and reached half maximum within 35 min. The slower gelation might be due to the mutual steric hindrance between the HA and Col. The storage modulus of the IPN did plateau 1 h after mixing. The semi-IPN gelation started slightly slower than in the other three gels, which is indicated by the fact that the storage modulus of the semi-IPN became higher than the loss modulus 71 s after mixing (Figure 2d). The storage modulus of the semi-IPN reached half maximum at around 38 min upon mixing and plateaued 1 h after mixing. The gelation time of the semi-IPN and IPN was very similar.

The storage moduli of all gels were frequency independent (Figure 2e), which indicates complete gelation. The storage modulus was larger than the loss modulus over the entire frequency range for all gels, which means the gels were viscoelastic solids.[31] The storage moduli of the IPN (2.5% xHA and 0.15% xCol) were approximately 1000 Pa, which was 15-fold larger than that of 0.3% xCol, 1.6-fold larger than that of semi-IPN but 5-fold smaller than that of 5% xHA. Generally, the storage moduli of the same hydrogels increase with their polymer concentration, so the storage modulus of the IPN can be further increased by adding more HA, which is the major component responsible for increasing mechanical strength in this system. However, in this study, to maintain a high water content, lower polymer content is desired. Hence, we chose to add 2.5% HA in the IPN gel to balance strength and high water content. Moreover, the IPN showed a larger storage modulus but a smaller loss modulus than the semi-IPN with the exact same polymer concentrations but nonchemically cross-linked Col. Therefore, the IPN was less viscous and could dissipate less energy as heat than the semi-IPN. The loss modulus of the IPN was more like that of xCol at lower frequencies and becomes closer to that of xHA at higher frequencies (Figure 2e).

3.3. Morphology.

The morphology of the IPN was compared to that of the xCol, xHA, and semi-IPN to verify the interpenetrating network formation. All gels were flash-frozen and lyophilized for SEM examination (Figure 3). The xCol gel had a relatively smooth surface with ridges at different magnifications (Figure 3a,b). On the other hand, the xHA exhibited a porous or pitted surface (Figure 3c,d).[32] The semi-IPN maintained porous features but the pores were larger than those of xHA (Figure 3e,f), suggesting that the nonchemically cross-linked Col and xHA were not fully interpenetrated with each other. In contrast to the semi-IPN, the IPN showed a surface morphology different from both the xCol and xHA but kept the ridge features of the xCol and the pitted features of the xHA (Figure 3g,h). These surface morphology changes suggested that the xHA and xCol were fully interpenetrated with each other and formed an interpenetrating network. Moreover, the IPN surface showed very similar features to the top view of the surface of the de-epithelialized rabbit cornea (Figure 3i,j). This finding was suggestive that the IPN surface could serve as a suitable substrate for corneal epithelial cells.

3.4. Transmittance and Refractive Index.

Next, we investigated the transmittance of the gels over time and the results are shown in Figure 4a. Promisingly, the freshly made IPN had a high transmittance (over 94%) for the entire visible spectrum from 380 to 740 nm. The transmittance decreased slightly on day 1 and day 3. Noticeably, the transmittance of the IPN on day 3 was very close to that on day 1. The high and stable transmittance of the IPN was expected because both xCol and xHA had high and stable transmittance. The semi-IPN, on the other hand, exhibited a low and unstable transmittance which was also seen in one of its components—the physically cross-linked Col. Therefore, the IPN was more promising than the semi-IPN as a corneal defect filler, which should be highly transparent to let the light go through and be received by the posterior eye.

Another important optical parameter of a corneal defect filler is its refractive index, which together with the surface curvature radius determines the focal power.[33] All gels in this study showed a lower refractive index than the human cornea (1.376),[34] which is to be expected given their higher water content. The refractive index of the IPN gel was 1.341, higher than that of 0.15% xCol (1.335) and semi-IPN (1.339) but lower than that of the 2.5% xHA (1.342) (Figure 4b). One method to increase the refractive index is to increase the polymer concentration. We first investigated the refractive index dependence on the homopolymer concentration with xHAs. Results showed that the refractive index of the xHA was linearly related to the concentration of HA with a Pearson's correlation coefficient of 0.9959 (Figure 4c). Based on the relationship between the refractive index and HA concentration shown in Figure 4c, 45.25% HA was required to reach the refractive index of the human cornea. On the other hand, when the xCol, xHA, semi-IPN, and IPN were studied together, we found that the refractive index was still linearly dependent on polymer concentration (Figure 4d). The Person's correlation coefficient was 0.9367. Based on this new relationship, 28.71% polymer content are needed to reach the refractive index of the human cornea at the time of application which is similar to the dry weight of the cornea. However, we expect that the gel will be degraded and remodeled over time and be deturgesced to some degree by the corneal endothelial pump. Thus, we do not believe that matching the corneal refractive index is critical for a transient, regenerative scaffold acting as a stromal defect filler.

3.5. Biocompatibility.

Both Col and HA are biocompatible naturally occurring macromolecules. However, functionalization could decrease their biocompatibility depending on the reactivity of the functional groups. Figure 5 shows the survival of corneal epithelial cells co-incubated with gel components after 4 h. Cell survival normalized to cell-only groups was 99, 98, 90, and 78% when cells were incubated with Col-azide, Col-DBCO, HA-MA, and HA-SH, respectively. The decrease in survival was not significant for all four gel components. The low cell survival in the presence of HA-SH was likely due to the presence of free thiol groups.[35] According to the literature, hydrogen peroxide could be produced during the thiol oxidation and lead to toxicity to cells.[36] This could be addressed if the cross-linked HA-SH showed a low cellular toxicity.

To this end, we studied the biocompatibility of the cross-linked gels with a live/dead assay and the results are shown in Figure 5b. The xCol (0.15%), xHA (2.5%), IPN, and semi-IPN all enabled cell survival over 80%, similar to that of the non-crosslinked Col, which indicated good biocompatibility of the gels. However, fluorescence microscopy revealed that the cell confluency on top of the IPN and semi-IPN was much higher than that of the xCol and xHA (Figure 5c). This result showed that the IPN combined the excellent cell adhesive property of Col and the strong mechanical property of HA, both of which improved the IPN gel's capacity for supporting corneal epithelial cell growth.

3.6. Corneal Stromal Defect Healing.

Ex vivo studies of gels filling anterior keratectomies in rabbit corneas demonstrated that the IPN could completely fill the corneal defect and restore the curvature of the cornea (Figure

6a). The IPN could fill small irregularities in the corneal defects because it was added in a flowable liquid state before gelling. The curvature restoration was very likely due to the similar surface tension between the native corneal stromal tissue and the IPN, both of which have very high water content.

The IPN remained clear during the first week after placement within the corneal stromal defects *in vivo*, while the untreated cornea became hazy on day 7 (Figure 6b). OCT showed that the IPN was slightly dehydrated on day 4 and there were no significant differences in the corneal thickness of the keratectomy areas of the IPN-treated and untreated corneas (Figure 6c). However, immunofluorescence studies showed substantial differences in the biological response to the treated and untreated areas. For the IPN-treated cornea, the IPN gel (red) was admixed with F-actin-expressing stromal cells and supported an overlying epithelium of 4–5 cell layers (Figure 6d). The epithelium overlying the IPN was similar to the normal epithelium and had a cuboidal basal cell layer underlying the anterior 3–4 layers of flattened superficial cells on day 7. However, the cuboidal basal cell layer on top of the IPN was less dense than that of the normal, untreated epithelium. Of note, the IPN treatment did not cause epithelial hyperplasia as was observed in the untreated cornea which had 15–20 layers of epithelial cells (Figure 6d).

Injured corneas showed F-actin-expressing cells beneath the epithelium (Figure 6d), while the normal cornea did not. These F-actin-expressing cells are likely activated myofibroblasts differentiated from stromal keratocytes. This activation of stromal cells is expected because it is one of the stages of wound healing.[37] To confirm this, we stained the tissue slices with alpha smooth muscle actin (α-SMA). Our results showed that the untreated cornea had more α-SMA expression below the regenerated epithelium than the IPN-treated corneas did (Figure 6e). Therefore, the IPN appeared to reduce myofibroblastic activity, which could lead to corneal haze and scarring. Both regenerated epithelia on IPN-treated and untreated corneas expressed the tight junction protein zonula occludens-1 (ZO-1), with the IPN-treated corneas showing higher ZO-1 expression than the untreated corneas (Figure 6f). The decreased α-SMA expression and increased ZO-1 expression seen in the IPN-treated corneas suggest that the *in situ*-forming, simultaneous IPN of Col and HA holds promise as a functional regenerative defect filler for the cornea.[38]

4. CONCLUSIONS

In this study, we reported on a natural biomacromolecule-based, *in situ*-forming simultaneous (one-pot) IPN hydrogel and evaluated its potential as a corneal defect filler to treat corneal stromal injuries. The IPN exhibited excellent biocompatibility because of the use of HA and Col and the use of dual and noncompeting cross-linking strategies in thiol–ene and bio-orthogonal SPAAC-based click chemistries. The IPN gels have high water content and maintained high and stable transparency over one week *in vivo*. The IPN combines the advantages of HA and Col, overcoming many of their individual shortcomings. The Col network conferred cell adhesivity, while HA conferred improved mechanical properties. The IPN could be applied to a corneal defect in a flowable liquid state and then form a smooth contour on its surface as it gels. Lastly, *in vivo* studies showed that the IPN treatment promotes epithelial overgrowth, promotes tight junction formation in the

epithelium, and decreases myofibroblast activity in the wounded stroma. Future studies will involve longer-term *in vivo* studies of the corneal wound healing response to this *in situ*-forming, simultaneous Col-HA IPN.

Acknowledgments

Funding

This work was supported by the National Institutes of Health (National Eye Institute K08EY028176 and a Departmental P30-EY026877 core grant), the Stanford SPARK Translational Research Grant and Maternal & Child Health Research Institute (MCHRI) (D.M.), a core grant and Career Development Award from Research to Prevent Blindness (RPB), the Matilda Ziegler Foundation, the VA Rehabilitation Research and Development Small Projects in Rehabilitation Effectiveness (SPiRE) program (I21 RX003179), and the Byers Eye Institute at Stanford. Part of this work was performed at the Stanford Nano Shared Facilities (SNSF), supported by the National Science Foundation under award ECCS-1542152.

ABBREVIATIONS

IPN	interpenetrating polymer network
HA	hyaluronic acid
xHA	thiol–ene click cross-linked hyaluronic acid
HA-SH	thiolated hyaluronic acid
HA-MA	methacrylated hyaluronic acid
SPAAC	strain-promoted azide–alkyne cycloaddition
Col	collagen
xCol	SPAAC click cross-linked collagen
DBCO	dibenzocyclooctyne
Col-azide	collagen modified with azido
Col-DBCO	collagen modified with DBCO
NC	neutralized collagen
PEG	poly(ethylene glycol)
NHS	*N*-hydroxysuccinimidyl ester
SEM	scanning electron microscopy
OCT	optical coherence tomography
ZO-1	zonula occludens-1
α-SMA	alpha smooth muscle actin
DAPI	4′,6-diamidino-2-phenylindole
PBS	phosphate buffered saline

REFERENCES

(1). Abdelkader A; Elewah E-SM; Kaufman HE Confocal Microscopy of Corneal Wound Healing After Deep Lamellar Keratoplasty in Rabbits. Arch. Ophthalmol 2010, 128, 75–80. [PubMed: 20065221]

(2). Gain P; Jullienne R; He Z; Aldossary M; Acquart S; Cognasse F; Thuret G Global Survey of Corneal Transplantation and Eye Banking. JAMA Ophthalmol. 2016, 134, 167–173. [PubMed: 26633035]

(3). Lee HJ; Fernandes-Cunha GM; Na KS; Hull SM; Myung D Bio-Orthogonally Crosslinked, In Situ Forming Corneal Stromal Tissue Substitute. Adv. Healthcare Mater 2018, 7, 1800560.

(4). Sani ES; Kheirkhah A; Rana D; Sun ZM; Foulsham W; Sheikhi A; Khademhosseini A; Dana R; Annabi N Sutureless repair of corneal injuries using naturally derived bioadhesive hydrogels. Sci. Adv 2019, 5, No. eaav1281. [PubMed: 30906864]

(5). Islam MM; Buznyk O; Reddy JC; Pasyechnikova N; Alarcon EI; Hayes S; Lewis P; Fagerholm P; He C; Iakymenko S; Liu W; Meek KM; Sangwan VS; Griffith M Biomaterials-enabled cornea regeneration in patients at high risk for rejection of donor tissue transplantation. npj Regener. Med 2018, 3, 2.

(6). Li L; Lu C; Wang L; Chen M; White J; Hao X; McLean KM; Chen H; Hughes TC Gelatin-Based Photocurable Hydrogels for Corneal Wound Repair. ACS Appl. Mater. Interfaces 2018, 10, 13283–13292. [PubMed: 29620862]

(7). Xu H-L; Tong M-Q; Wang L-F; Chen R; Li X-Z; Sohawon Y; Yao Q; Xiao J; Zhao Y-Z Thiolated γ-polyglutamic acid as a bioadhesive hydrogel-forming material: evaluation of gelation, bioadhesive properties and sustained release of KGF in the repair of injured corneas. Biomater. Sci 2019, 7, 2582–2599. [PubMed: 30977482]

(8). Kenne L; Gohil S; Nilsson EM; Karlsson A; Ericsson D; Helander Kenne A; Nord LI Modification and cross-linking parameters in hyaluronic acid hydrogels–definitions and analytical methods. Carbohydr. Polym 2013, 91, 410–418. [PubMed: 23044151]

(9). Kim SJ; Lee CK; Lee YM; Kim IY; Kim SI Electrical/pH-sensitive swelling behavior of polyelectrolyte hydrogels prepared with hyaluronic acid-poly(vinyl alcohol) interpenetrating polymer networks. React. Funct. Polym 2003, 55, 291–298.

(10). Burdick JA; Prestwich GD Hyaluronic Acid Hydrogels for Biomedical Applications. Adv. Mater 2011, 23, H41–H56. [PubMed: 21394792]

(11). Neuman MG; Nanau RM; Oruña-Sanchez L; Coto G Hyaluronic acid and wound healing. J. Pharm. Pharm. Sci 2015, 18, 53–60. [PubMed: 25877441]

(12). Zhong J; Deng Y; Tian B; Wang B; Sun Y; Huang H; Chen L; Ling S; Yuan J Hyaluronate acid-dependent protection and enhanced corneal wound healing against oxidative damage in corneal epithelial cells. J. Ophthalmol 2016, 2016, 6538051. [PubMed: 27190638]

(13). Fernandes-Cunha GM; Na KS; Putra I; Lee HJ; Hull S; Cheng YC; Blanco IJ; Eslani M; Djalilian AR; Myung D Corneal Wound Healing Effects of Mesenchymal Stem Cell Secretome Delivered Within a Viscoelastic Gel Carrier. Stem Cells Transl. Med 2019, 8, 478. [PubMed: 30644653]

(14). Lee HJ; Fernandes-Cunha GM; Myung D In situ-forming hyaluronic acid hydrogel through visible light-induced thiol-ene reaction. React. Funct. Polym 2018, 131, 29–35. [PubMed: 32256185]

(15). Rýglová Š; Braun M; Suchý T Collagen and Its Modifications—Crucial Aspects with Concern to Its Processing and Analysis. Macromol. Mater. Eng 2017, 302, 1600460.

(16). Suri S; Schmidt CE Photopatterned collagen–hyaluronic acid interpenetrating polymer network hydrogels. Acta Biomater. 2009, 5, 2385–2397. [PubMed: 19446050]

(17). Naseri N; Deepa B; Mathew AP; Oksman K; Girandon L Nanocellulose-Based Interpenetrating Polymer Network (IPN) Hydrogels for Cartilage Applications. Biomacromolecules 2016, 17, 3714–3723. [PubMed: 27726351]

(18). Jeon O; Shin J-Y; Marks R; Hopkins M; Kim T-H; Park H-H; Alsberg E Highly Elastic and Tough Interpenetrating Polymer Network-Structured Hybrid Hydrogels for Cyclic Mechanical Loading-Enhanced Tissue Engineering. Chem. Mater 2017, 29, 8425–8432.

(19). Gong JP; Katsuyama Y; Kurokawa T; Osada Y Double-Network Hydrogels with Extremely High Mechanical Strength. Adv. Mater 2003, 15, 1155–1158.

(20). Myung D; Waters D; Wiseman M; Duhamel P-E; Noolandi J; Ta CN; Frank CW Progress in the development of interpenetrating polymer network hydrogels. Polym. Adv. Technol 2008, 19, 647–657. [PubMed: 19763189]

(21). Myung D; Koh W; Ko J; Hu Y; Carrasco M; Noolandi J; Ta CN; Frank CW Biomimetic strain hardening in interpenetrating polymer network hydrogels. Polymer 2007, 48, 5376–5387.

(22). Hodgson SM; Bakaic E; Stewart SA; Hoare T; Adronov A Properties of Poly(ethylene glycol) Hydrogels Cross-Linked via Strain-Promoted Alkyne–Azide Cycloaddition (SPAAC). Biomacromolecules 2016, 17, 1093–1100. [PubMed: 26842783]

(23). Madl CM; Katz LM; Heilshorn SC Bio-Orthogonally Crosslinked, Engineered Protein Hydrogels with Tunable Mechanics and Biochemistry for Cell Encapsulation. Adv. Funct. Mater 2016, 26, 3612–3620. [PubMed: 27642274]

(24). Leonard BC; Cosert K; Winkler M; Marangakis A; Thomasy SM; Murphy CJ; Jester JV; Raghunathan VK Stromal Collagen Arrangement Correlates with Stiffness of the Canine Cornea. Bioengineering 2019, 7, 4.

(25). Highley CB; Prestwich GD; Burdick JA Recent advances in hyaluronic acid hydrogels for biomedical applications. Curr. Opin. Biotechnol 2016, 40, 35–40. [PubMed: 26930175]

(26). Hoyle CE; Bowman CN Thiol–Ene Click Chemistry. Angew. Chem., Int. Ed 2010, 49, 1540–1573.

(27). Griffith GL; Wirostko B; Lee H-K; Cornell LE; McDaniel JS; Zamora DO; Johnson AJ Treatment of corneal chemical alkali burns with a crosslinked thiolated hyaluronic acid film. Burns 2018, 44, 1179–1186. [PubMed: 29429747]

(28). Gwon K; Kim E; Tae G Heparin-hyaluronic acid hydrogel in support of cellular activities of 3D encapsulated adipose derived stem cells. Acta Biomater. 2017, 49, 284–295. [PubMed: 27919839]

(29). Zhang Y; Liu S; Li T; Zhang L; Azhar U; Ma J; Zhai C; Zong C; Zhang S Cytocompatible and non-fouling zwitterionic hyaluronic acid-based hydrogels using thiol-ene “click” chemistry for cell encapsulation. Carbohydr. Polym 2020, 236, 116021. [PubMed: 32172841]

(30). Kharkar PM; Rehmann MS; Skeens KM; Maverakis E; Kloxin AM Thiol–ene Click Hydrogels for Therapeutic Delivery. ACS Biomater. Sci Eng 2016, 2, 165–179. [PubMed: 28361125]

(31). Zhou J; Wang G; Zou L; Tang L; Marquez M; Hu Z Viscoelastic behavior and in vivo release study of microgel dispersions with inverse thermoreversible gelation. Biomacromolecules 2008, 9, 142–148. [PubMed: 18067257]

(32). Cui L; Xiong Z; Guo Y; Liu Y; Zhao J; Zhang C; Zhu P Fabrication of interpenetrating polymer network chitosan/gelatin porous materials and study on dye adsorption properties. Carbohydr. Polym 2015, 132, 330–337. [PubMed: 26256356]

(33). Olsen GH On the Calculation of Power from Curvature of the Cornea. Br. J. Ophthalmol 1986, 70, 152–154. [PubMed: 3947615]

(34). Wang L; Mahmoud AM; Anderson BL; Koch DD; Roberts CJ Total Corneal Power Estimation: Ray Tracing Method versus Gaussian Optics Formula. Invest. Ophthalmol. Vis. Sci 2011, 52, 1716–1722. [PubMed: 21071742]

(35). Deshpande A; Bhatia M; Laxman S; Bachhawat A Thiol trapping and metabolic redistribution of sulfur metabolites enable cells to overcome cysteine overload. Microb. Cell 2017, 4, 112–126. [PubMed: 28435838]

(36). Held KD; Biaglow JE Mechanisms for the oxygen radical-mediated toxicity of various thiol-containing compounds in cultured mammalian cells. Radiat. Res 1994, 139, 15–23. [PubMed: 8016303]

(37). Chen J; Li Z; Zhang L; Ou S; Wang Y; He X; Zou D; Jia C; Hu Q; Yang S; Li X; Li J; Wang J; Sun H; Chen Y; Zhu YT; Tseng SCG; Liu Z; Li W Descemet’s Membrane Supports Corneal Endothelial Cell Regeneration in Rabbits. Sci. Rep 2017, 7, 6983. [PubMed: 28765543]

(38). Sugrue SP; Zieske JD ZO1 in Corneal Epithelium: Association to the Zonula Occludens and Adherens Junctions. Exp. Eye Res 1997, 64, 11–20. [PubMed: 9093016]

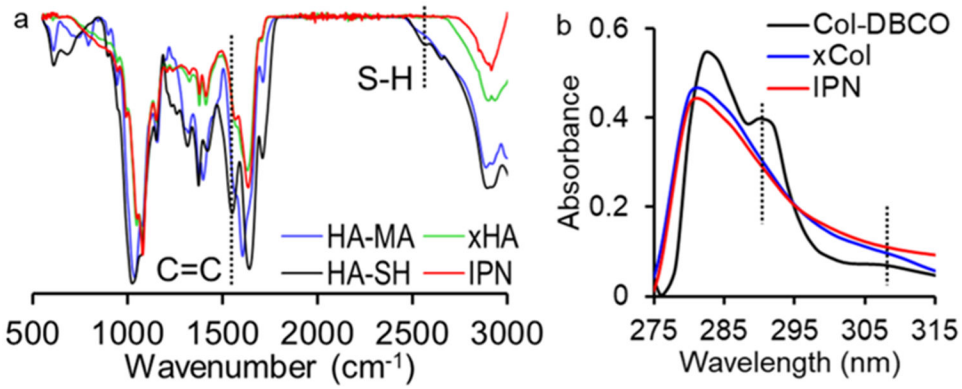

Figure 1.

Evidence of formation of xHA and xCol in the IPN gel. (a) FTIR spectra of HA-MA, HA-SH, xHA, and IPN. The absence of S–H and C═C signals in the IPN and xHA spectra indicates the cross-linking between thiol and methacrylate groups in both gels. (b) UV–vis spectra of Col-DBCO, xCol, and IPN. The absence of absorbance peaks at around 290 and 310 nm in both the xCol and IPN indicates that the DBCO has been reacted.

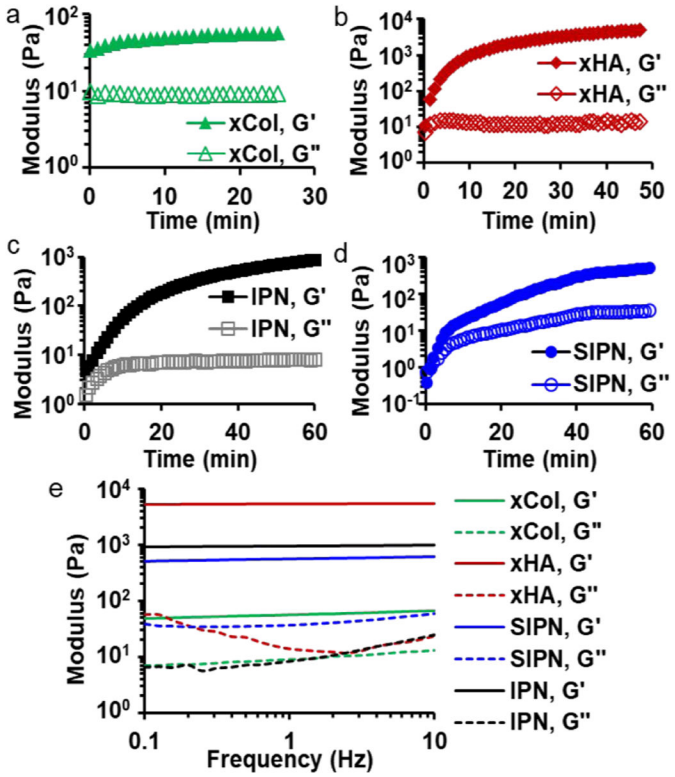

Figure 2.

Rheological characterizations of gels. *In situ* rheology measurements indicate the gelation time of the four types of gels: (a) Col SPAAC gel with 0.3% Col; (b) xHA with 5% HA; (c) IPN with 0.15% xCol and 2.5% xHA; (d) semi-IPN with 0.15% neutralized Col and 2.5% xHA. G' and G'' represent storage and loss modulus, respectively. (e) Dynamic moduli of gels as a function of frequency. All gels exhibited a viscoelastic solid-like state as the storage moduli were larger than the loss moduli.

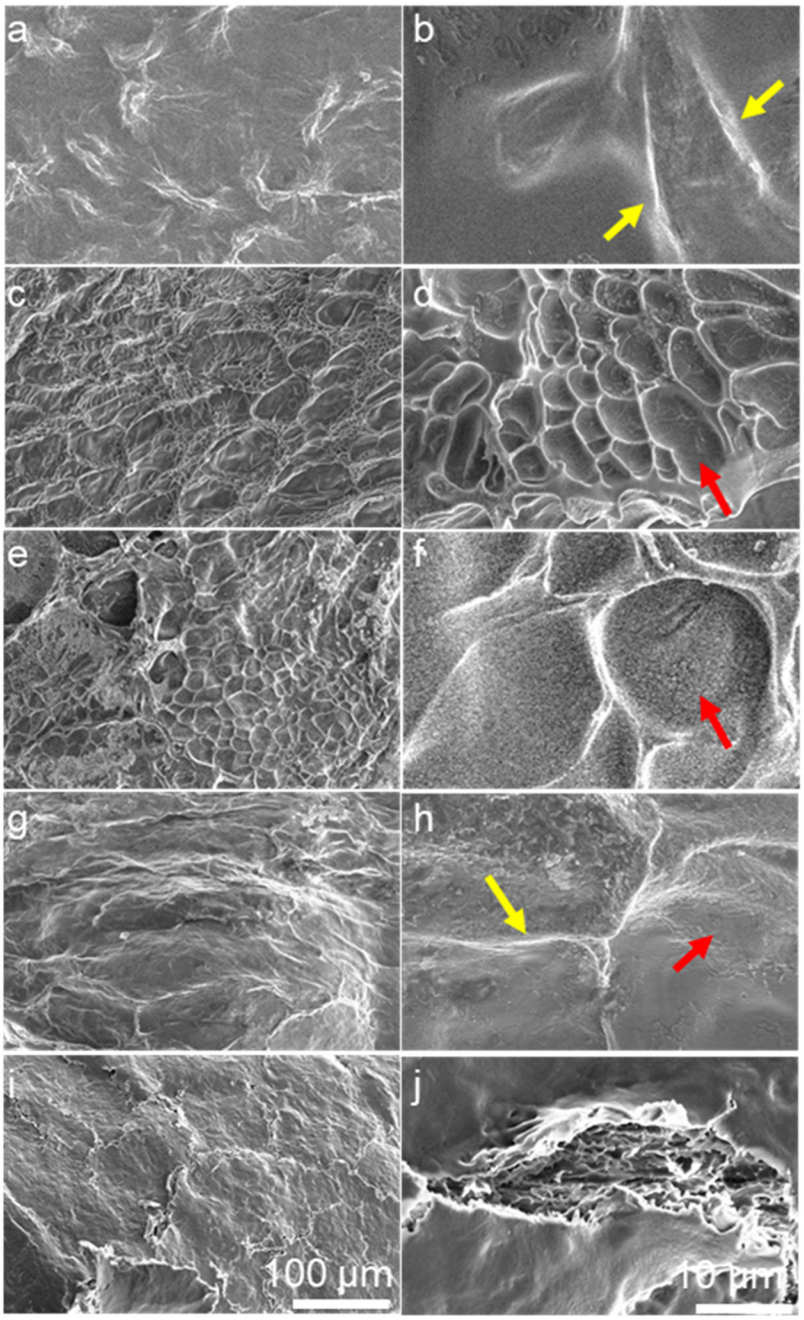

Figure 3.

SEM morphology of gels and de-epithelialized cornea. (a,b) xCol 0.3% Col showed ridges (yellow arrow) on the surface. (c,d) xHA with 5% HA showed pits (red arrow) on the surface. (e,f) Semi-IPN with 0.15% neutralized Col and 2.5% xHA. (g,h) IPN with 0.15% xCol and 2.5% xHA showed both ridges and pits. (i,j) de-epithelialized rabbit cornea. All samples were flash-frozen and lyophilized for SEM imaging. The scale bar of panels (a,c,e,g) is the same as that of panel (i), and the scale bar of panels (b,d,f,h) is the same as that of panel (j).

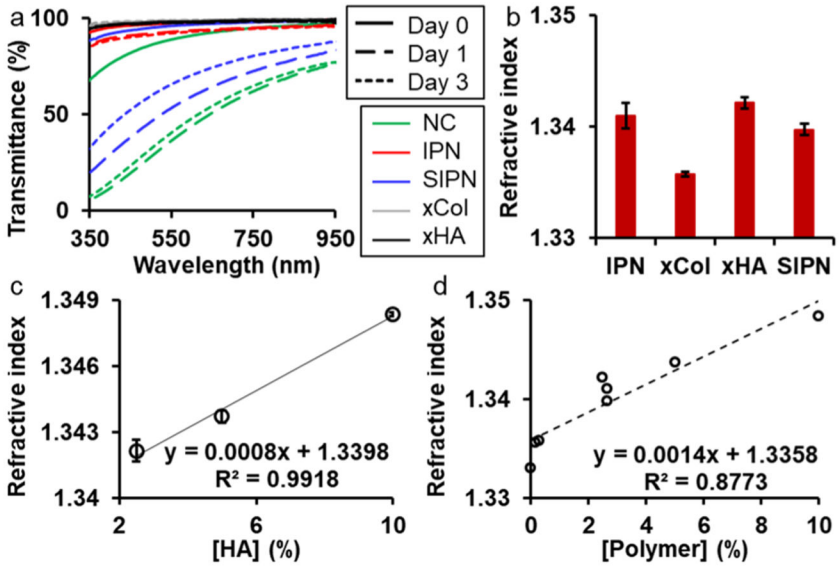

Figure 4.

Transmittance and refractive index of the gels. (a) Transmittance of hydrogels over time. (b) Refractive indices of the four types of gels. (c) Refractive index of xHA with different HA concentrations. (d) Relationship between the refractive index and total polymer concentrations. NC: nonchemically cross-linked Col; IPN: 0.15 xCol and 2.5% xHA; semi-IPN: 0.15 Col and 2.5% xHA; xCol: 0.15% Col; and xHA: 2.5% HA.

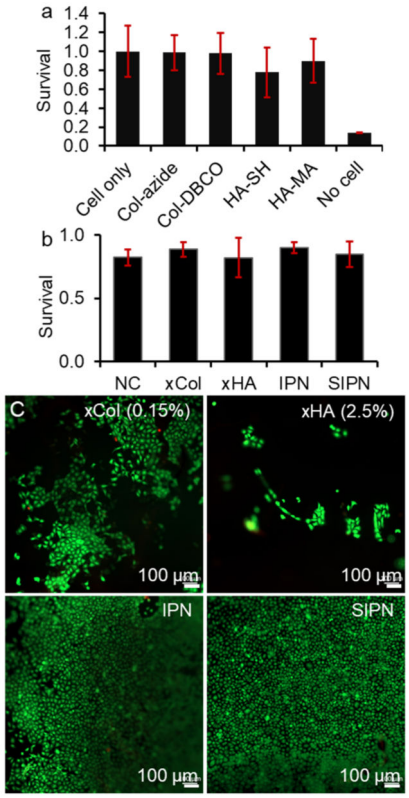

Figure 5.

Biocompatibility of the gel components and the gels. (a) Resazurin assay showed the corneal epithelial cell survival in the presence of gel components. (b) calcein AM/ethidium homodimer-I live/dead assay showed the corneal epithelial cell survival on top of gels. (c) Representative fluorescence images of cells on top of gels. IPN: 0.15 xCol and 2.5% xHA; semi-IPN: 0.15 Col and 2.5% xHA; xCol: 0.15% Col; and xHA: 2.5% HA.

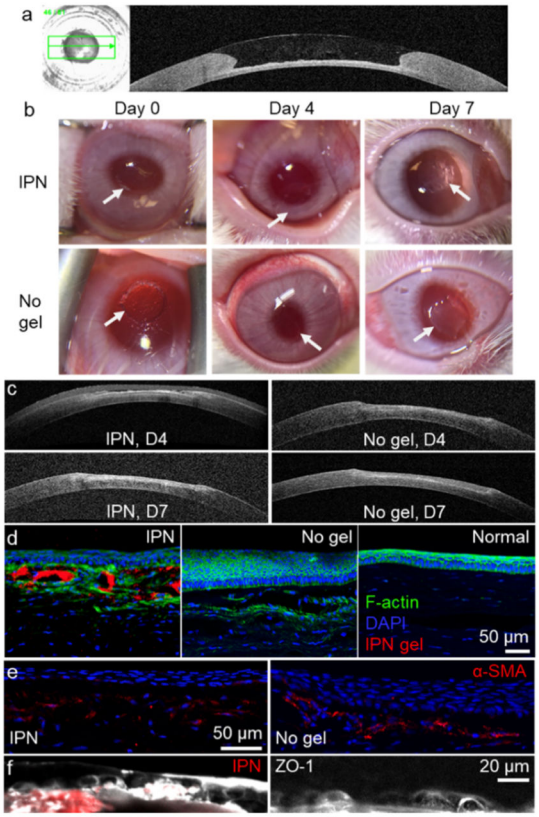

Figure 6.

Ex vivo and *in vivo* studies of the application of the IPN as a corneal defect filler. (a) OCT image shows the curvature restoration of the IPN on a rabbit corneal defect *ex vivo*. The IPN was added to the corneal defect when it is still in a liquid-like state. (b) Magnified photos of treated eyes on different days after treatment. The keratectomy area of the untreated group was more opaque than that treated with the IPN. The arrows indicate the edges of the keratectomy area. (c) OCT images of corneal defect recovery over 1 week. Immunofluorescence staining of regenerated anterior corneal tissues: (d) F-actin, (e) alpha smooth muscle actin, and (f) zonula occludens-1. Images on the same row share the same scale bar.

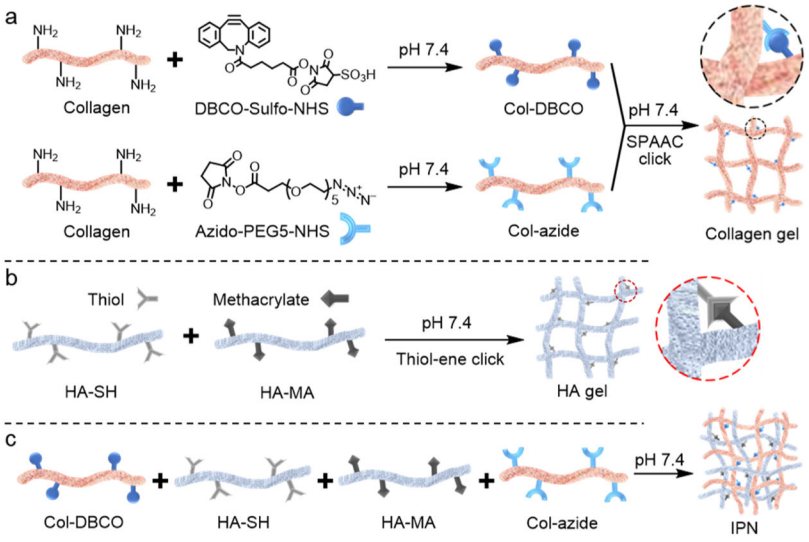

Scheme 1.

Formation of the HA and Col-Based IPN; (a) Col was Modified with DBCO-sulfo-NHS and Azido-PEG5-NHS; Modified Cols were Then Mixed and Cross-linked *via* Bio-Orthogonal SPAAC under Physiological Conditions; Col SPAAC Click Gel is Denoted as xCol; (b) xHA was Formed by Cross-linking HA-SH and HA-MA *via* Thiol–Ene Click Reaction under Physiological Conditions; and (c) DBCO-modified Col, HA-SH, HA-MA, and Azido-Modified Col were Mixed in Order to Form the IPN under Physiological Conditions

Table 1.

Polymer Content of the Hydrogels in This Study

gel	Col content (%)	HA content (%)
xCol	0.15, 0.3	0
xHA	0	2.5, 5, 10
semi-IPN	0.15[a]	2.5
IPN	0.15	2.5

[a]No chemical cross-linking.